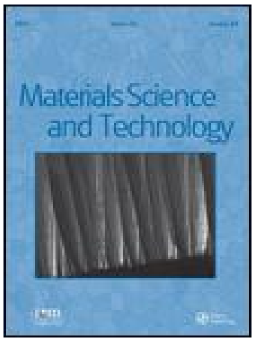

Materials Science and Technology

ISSN: 0267-0836 (Print) 1743-2847 (Online) Journal homepage: https://www.tandfonline.com/loi/ymst20

Wetting behaviour and interfacial microstructure of Sn–Ag–Zn solder alloys on nickel coated aluminium substrates

Satyanarayan & K N Prabhu

To cite this article: Satyanarayan & K N Prabhu (2011) Wetting behaviour and interfacial microstructure of Sn–Ag–Zn solder alloys on nickel coated aluminium substrates, Materials Science and Technology, 27:7, 1157-1162, DOI: 10.1179/026708310X12815992418337

To link to this article: https://doi.org/10.1179/026708310X12815992418337

Wetting behaviour and interfacial microstructure of Sn–Ag–Zn solder alloys on nickel coated aluminium substrates

Satyanarayan and K. N. Prabhu*

Wetting behaviours of two lead free solders (Sn–2·625Ag–2·25Zn and Sn–1·75Ag–4·5Zn) on nickel coated aluminium substrates were investigated. Sn–2·625Ag–2·25Zn exhibited better wettability compared to Sn–1·75Ag–4·5Zn solder. Contact angles of the solders increased with increasing roughness of the substrate. The Young–Dupre equation was used to evaluate the work of adhesion of solder on the substrate. Sn–2·625Ag–2·25Zn solder exhibited higher work of adhesion than Sn–1·75Ag–4·5Zn. A thin continuous layer of Ni_3Sn was detected at the interface between Sn–2·625Ag–2·25Zn solder and nickel coated Al substrate. Sn–1·75Ag–4·5Zn solder exhibited scallop intermetallic compounds (IMCs) growing into the solder field as well as a thin continuous IMC in some cases. Ni_3Sn and Ni_3Sn_4 IMCs were observed at the interface of Sn–1·75Ag–4·5Zn solder and nickel coated Al.

Keywords: Lead free solders, Contact angle, Wettability, Work of adhesion, IMCs

Introduction

Sn–Pb solders are widely used in printed circuit boards (PCBs). However, the lead present in solders is hazardous to human beings and not ecofriendly.[1,2] Lead free solders are therefore increasingly being used in electronic applications. For the last two decades, a lot of research work has been carried out to prepare and characterise lead free solders having properties close to the Sn–37Pb solder.[1–6] Lead free solder materials must emulate the broad range of properties and characteristics of the lead based solders for their successful use in electronic assemblies. The basic soldering process depends on wetting for the formation of solder to base metal contact.[7] The solidification of molten solder after wetting results in permanent bond.[7,8] Therefore, the new solders (binary and ternary) must wet and bond to metallic terminals/substrates or components and must have a melting point that is sufficiently low to be reflowed as a paste attaching metallic terminals or PCBs.

Eutectic Sn–Ag, Sn–Ag–Cu, Sn–In and Sn–Bi solders have emerged as candidate materials[1,6,9,10] to replace the Sn–37Pb solder due to their better ductility, creep resistance and thermal resistance properties.[6] Owing to the higher melting point and poor wettability of Sn–Ag solders[1,2,4,9,11] as compared to Sn–Pb solders, introduction of alloying elements, such as Cu, Ni, In, Bi and Zn have been made to reduce the melting point of eutectic Sn–3·5Ag solder and simultaneously improve its mechanical properties.[1,4]

The presence of Zn in the Sn–Ag solder results not only in a decrease in its melting point but also in the significant improvement of its mechanical properties.[4,12] Furthermore, the formation of Ag–Zn intermetallic compounds (IMCs) is beneficial to improve the resistance of corrosion together with a comparable wetting ability.[11] The nature of bond formation depends on the solder alloy composition and the type of metallic substrate used for soldering application.[9] The selection of the substrate plays a vital role in electronic application. Cu, Ni, Au and Pd are the common substrate materials used in electronic applications.[13–15]

There is no solder which operates with aluminium in the same way that ordinary solders operate with copper. Because Al does not alloy readily with solders at temperatures as low as the other metal require,[16] it is necessary to use a much higher temperature. The Al surface is covered with a thin invisible coating aluminium oxide. Thin oxide film makes it difficult to solder the dissimilar materials.[16,17] Hence, in soldering aluminium, it is necessary that this oxide has to be removed before the soldering take place. Furthermore, the solder will not flow into an Al joint, even when oxide is removed, by capillary action as it does into copper.[16]

In the present work, pure aluminium substrate plated with Ni layer of 12 μm thickness is used as the soldering substrate. The wetting behaviours of two lead free solders, namely, Sn–2·625Ag–2·25Zn and Sn–1·75Ag–4·5Zn, on nickel coated Al substrates were investigated.

Experimental

Sn–2·625Ag–2·25Zn and Sn–1·75Ag–4·5Zn alloys were prepared using ingots of pure Sn–3·5 Ag and Sn–9Zn alloys. The melting was carried out in an electric

Department of Metallurgical and Materials Engineering, National Institute of Technology Karnataka, Surathkal, Mangalore 575 025, India

*Corresponding author, email prabhukn_2002@yahoo.co.in

Published by Maney on behalf of the Institute
Received 13 June 2010; accepted 23 July 2010
DOI 10.1179/026708310X12815992418337

resistance furnace to produce Sn–Ag–Zn solder alloy ingots with the composition as given in Table 1.

The ternary Sn–Ag–Zn alloy ingots were cut and drawn into solder (Sn–Ag–Zn) wires with a diameter of ~4 mm. Solder wire was melted using a solder station (KLAPP 920D) and solidified as balls of 0·080 g. The solder balls were then used for assessment of wettability and kinetics of spreading on nickel coated aluminium substrates. The Ni plating on Al was carried out at Modern Electroplaters (Mangalore, India). The coating thickness was ~12 μm. The surface roughness of coated substrates was measured using a Form Talysurf 50 surface profiler. Contact angle measurements were carried out using an FTA 200 dynamic contact angle analyser. An environmental chamber with heating element and temperature controller forms the accessory for melting the solder ball on the substrate for wetting tests. The system can capture both static and dynamic spreading phenomena. The initial heating rate obtained with the chamber is about 3–4 K min^{-1}, which eventually reduces as the chamber temperature approaches the set value. Spherical balls of solder alloy were kept on the substrate, and the solder/substrate system was held inside the environmental chamber after coating with flux (inorganic acid; Alfa Aesar, Ward Hill, MA, USA). The chamber was heated to a temperature higher than the liquidus temperature of the solder alloy by ~40°C (241°C for Sn–2·625Ag–2·25Zn and 244°C for Sn–1·75Ag–4·5Zn solder) and maintained at that temperature during the entire process of spreading. Images were captured at regular time intervals after spreading has started. Initially, the images were captured at a rate of 0·0167 frames/s, and then, the time of interval of image capture was incremented by 0·5%. The spreading process is recorded for ~2420 s. The captured images were analysed using FTA 32 Video 2·0 software (First Ten Angstrom) to determine the wetting behaviour. Table 2 gives the experimental matrix.

The solder drop bonded to the substrate was sectioned along the axis and polished using SiC papers of different grit sizes. The final polishing was carried out on velvet cloth disc polisher using 1 μm levitated alumina and then etched with 5% nital. The solder/substrate interfacial region was microexamined using a Zeiss Axio Imager optical microscope as well as a JEOL JSM 6380LA scanning electron microscope (SEM). X-ray diffraction (XRD) study was carried out to identify and characterise the IMC at the solder/substrate interface. A JEOL JDX-8P-XRD system was used for this purpose.

Results and discussion

Wetting behaviour

The typical relaxation curves for spreading of Sn–2·625Ag–2·25Zn and Sn–1·75Ag–4·5Zn solder on Ni coated Al substrates with different surface roughnesses R_a are shown in Figs. 1 and 2 respectively. The decrease in contact angle relaxation was sharp at the initial stages, and it became gradual as the solidifying solder approached equilibrium. The liquid solder spreads rapidly in the beginning at a time of about 100–120 s with a sharp increase in base radius. The spreading of solder ceased after a time of about 900–1000 s. In the present study, the contact angle at which relaxation rate becomes $<0{\cdot}01^\circ\ s^{-1}$ was taken as the stabilised or equilibrium contact angle. Each spreading experiment of solder on substrate is carried out at least three times.

Table 1 Composition of Sn–Ag–Zn solder alloy

Constituent	Zn	Ag	Fe	Sn
Content, wt-%	2·25	2·62	<0·005	Bal.
	4·5	1·75	<0·005	

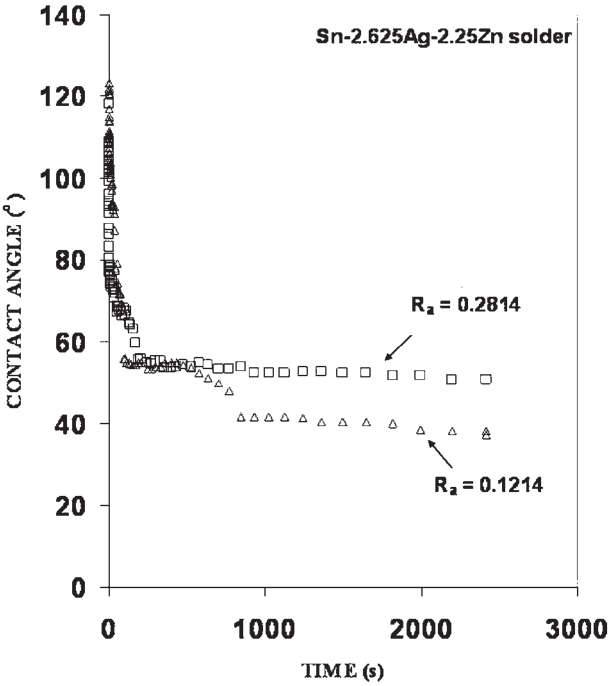

1 Relaxation behaviour of Sn–2·625Ag–2·25Zn solder on Ni coated Al substrates

Equilibrium contact angle values in the range of 34–50° were obtained for Sn–2·625Ag–2·25Zn solder on Ni coated Al substrates. For Sn–1·75Ag–4·5Zn solder, the contact angles were slightly higher and were in the range of 46–51°. Table 3 gives the values of static contact angles for Ni coated Al substrates having different surface textures. The contact angle increases with increasing surface texture on Ni coated Al substrates for both solders.

For qualitative evaluation of the above results, the Young–Dupre equation was used to calculate the work of adhesion. The work of adhesion is defined as the work that must be performed per unit area of the interface to separate the two phases. It is a measure of strength of binding between the phases. Dupre defined the work of adhesion between solid and liquid as

$$W_{sl} = \gamma_{sv} + \gamma_{lv} - \gamma_{sl} \quad (1)$$

Substituting this equation in Young's equation

Table 2 List of experiments

Solder alloys	Substrate	Roughness R_a, μm	Temperature ($T_M + \Delta T$), °C
Sn–2·625Ag–2·25Zn	Ni coat on Al	0·2814	241
		0·1214	
		0·1072	
Sn–1·75Ag–4·5Zn	Ni coat on Al	0·4881	244
		0·3509	
		0·2163	

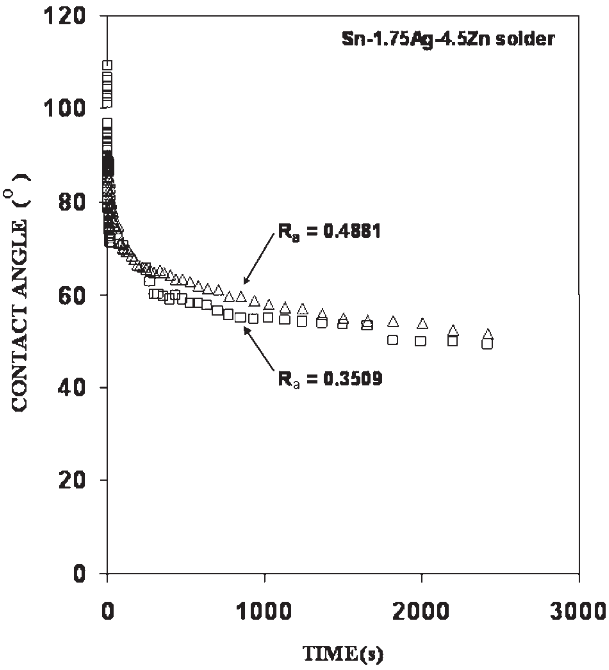

2 Relaxation behaviour of Sn–1·75Ag–4·5Zn solder on Ni coated Al substrates

$$\gamma_{sv} - \gamma_{sl} = \gamma_{lv} \cos\theta \tag{2}$$

yields the Young–Dupre equation

$$W_{sl} = \gamma_{lv}(1 + \cos\theta) \tag{3}$$

In the above equations, γ_{sv} is the interfacial energy between the phases solid and vapour. γ_{sl} is the interfacial energy between the phases solid and liquid. γ_{lv} is the interfacial energy between the phases liquid and vapour, and θ is the contact angle of the liquid solder. By inserting the value of contact angle and the surface tension of the liquid in the above equation, work of adhesion can be calculated. The surface tensions of Sn–3·5Ag and Sn–9Zn solders are reported as 431 and 518 mN m^{-1} respectively.[18] Since the solders used in the present investigation are prepared using these solders, weighted average values of surface tension are used in the present investigation for computing the work of adhesion. The calculated values of surface tension for Sn–2·625Ag–2·25Zn and Sn–1·75Ag–4·5Zn solders are 453·5 and 474 mN m^{-1} respectively.

Table 3 Effect of surface roughness on static contact angles of Sn–2·625Ag–2·25Zn and Sn–1·75Ag–4·5Zn solder on Ni coated Al substrates

	Sn–2·625Ag–2·25Zn		Sn–1·75Ag–4·5Zn	
Substrate	R_a, μm	θ, °	R_a, μm	θ, °
Ni coated aluminium	0·2814	50·63	0·4881	51·47
	0·1214	35·21	0·3509	49·21
	0·1072	34·92	0·2163	46·82

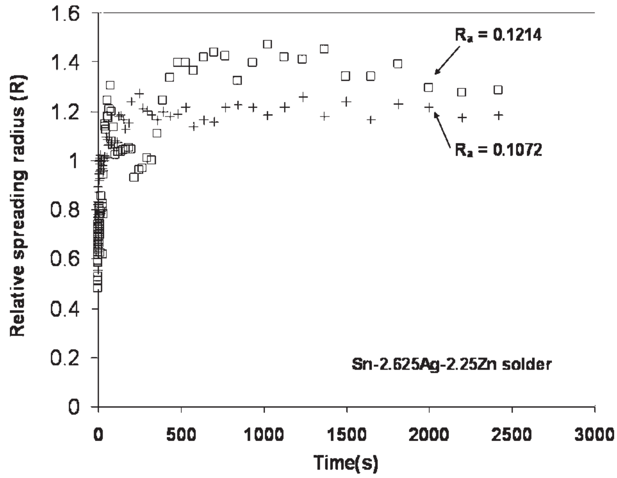

3 Effect of surface roughness on relative spreading radius of Sn–2·625Ag–2·25Zn solder on Ni coated Al substrate

Lower the value of contact angle will be the larger work of adhesion. There was no significant difference in the work of adhesion estimated for both alloys. Table 4 gives the calculated values of work of adhesion for both solders on Ni coated Al substrate. The work of adhesion is found to be higher for substrates having smooth surface.

Shimada *et al.*[19] indicated that the radius of the droplet depends on the amount of liquid solder and a relative spreading radius R was defined as $R = r/r_{sph}$. Here, r is the radius of the solder on substrate for each experiment, and r_{sph} is the radius of the hypothetical sphere having the same volume of the solder ball that was used during wetting experiment. From the mass and density of the solder ball, the volume and the radius r_{sph} were calculated. The relative spreading radius R indicates a value of $\sim$1·0 during soldering. The relative spreading radius increases with increasing time, and as the surface roughness R_a increases, the relative spreading also increases. The changes in $R = r/r_{sph}$ with time for both solders are shown in Figs. 3 and 4 respectively.

Solder/substrate interfacial microstructure

Plating aluminium with copper, nickel, silver or other high melting metals before soldering generally improves its resistance to corrosion.[16] During soldering of Sn–Ag–Zn alloy on pure Ni, Ni/Cu or Ni/Al, two physicochemical processes will occur. The first process is the dissolution of the solder alloy into the base metal, and the second is the formation of IMCs at the interface after molten solder wets the substrates.[20]

Table 4 Calculated values of work of adhesion of solders on substrates

Sn–2·625Ag–2·25Zn		Sn–1·75Ag–4·5Zn	
Roughness R_a, μm	Work of adhesion, mN m^{-1}	Roughness R_a, μm	Work of adhesion mN mm^{-1}
0·2814	741·1266	0·3509	785·272
0·1214	824·0087	0·2163	800·0023
0·1072	825·3278	0·4881	770·8458

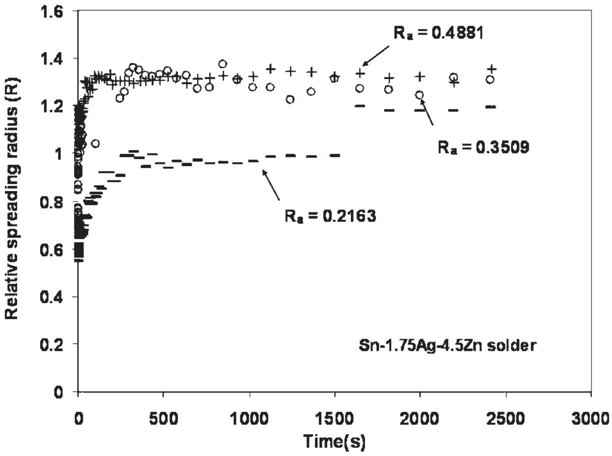

4 Effect of surface roughness on relative spreading radius of Sn–1·75Ag–4·5Zn solder on nickel coated Al substrate

Figures 5 and 6 represent the optical and SEM images of Sn–2·62Ag–2·25Zn and Sn–1·75Ag–4·5Zn solder/Ni coated aluminium. During soldering of Sn–2·625Ag–2·25Zn (at 241°C) and Sn–1·75Ag–4·5Zn (at 244°C), the molten solder reacts with the Ni layer first. An increase in the dissolution of liquid solder atoms in Ni layer results in IMCs at the interface. Here, the layer of Ni on Al assists in slowing down the diffusion of solder into the aluminium.

In the soldering period, solder atoms diffused into the Ni layer. This diffusion of solidifying liquid solder into Ni layer leads to IMC formation at the interface. Ni_3Sn, Ni_3Sn_2 and Ni_3Sn_4 IMCs are known to exist in the Ni–Sn binary system.[20,21] Figure 5*a* clearly shows the diffusion of solder into the nickel layer coated on the substrate. Figure 5*b* shows a thin continuous IMC layer (thin white layer marked as region A) at the interface. The elemental analysis of IMCs, formed at the interface between solder and the substrate, is given in Table 5.

The chemical composition (Table 5) at the interface (Fig. 5*b*, region A) shows tin rich phase with 18·58 at-%Ni, and small amount of Al and Ag dissolved in it, which is nearly in the Ni/Sn ratio of 3 : 1. This can be identified as Ni_3Sn compound that has formed at the interface. To identify the phase of IMC, XRD analysis was performed. Figure 7 shows the XRD pattern of Sn–2·625Ag–2·25Zn solder on Ni plated Al substrate interface. XRD pattern confirms the formation of Ni_3Sn IMC at the interface.

Figure 6*a* shows the interfacial microstructures of Sn–1·75Ag–4·5Zn on Ni coated Al. The microstructure shows that a scallop shaped IMC grown into the solder field has occurred at the interface. In some cases, the solder exhibited thin continuous IMC at the interface.

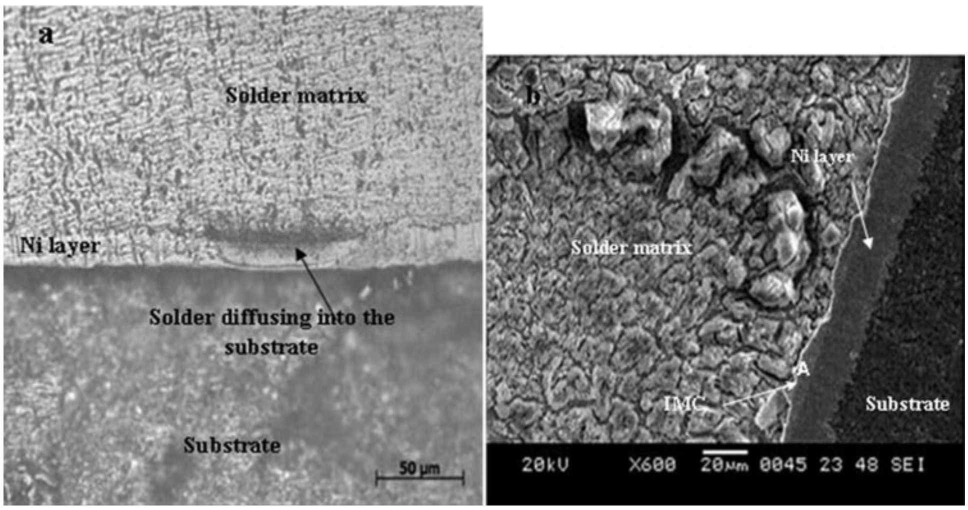

5 *a* microstructure and *b* SEM image of Sn–2·625Ag–2·25Zn solder/Ni coated aluminium

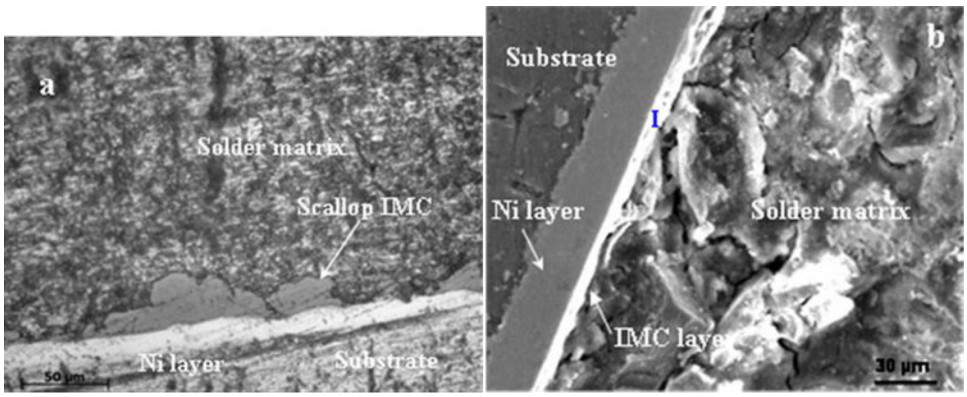

6 *a* microstructure and *b* SEM image of Sn–1·75Ag–4·5Zn solder/Ni coated aluminium

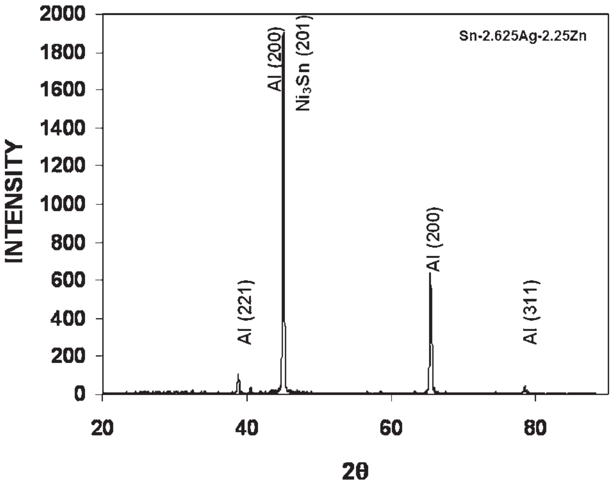

7 X-ray diffraction pattern of Sn–2·625Ag–2·25Zn/Ni coated Al interface

Figure 6*b* shows the SEM image of formation of thin continuous IMC layer (region I) at the interface.

The elemental analysis of region I (Fig. 6*b*) shows that the thin IMC layer is composed of 21·88 at-%Ni and 5·86 at-%Sn in the ratio of 3 : 1. This can be identified as Ni_3Sn IMC. Table 6 shows the elemental analysis at the interface.

Figure 8 shows the XRD pattern obtained for Sn–1·75Ag–4·5Zn solder on the Ni coated Al substrate indicating the formation of Ni_3Sn and Ni_3Sn_4 IMCs at the interface. The XRD patterns for both solders were similar in nature, but Sn–1·75Ag–4·5Zn solder showed occurrence of peaks corresponding to both Ni_3Sn as well as Ni_3Sn_4 IMC at the interface.

The wettability of Sn–1·75Ag–4·5Zn solder was poorer compared to Sn–2·625Ag–2·25Zn on Ni coated Al. For both solders, the spreading of solder was sharp at the beginning, and spreading almost ceases when it starts diffusing into the Ni. Nickel atoms and its

Table 5 Energy dispersive spectroscopy analysis results of (A region in Fig. 5*b*) Sn–2·625Ag–2·25Zn solder on Ni coated Al substrate

	Positions
Elements	Region A, at-%
Al K	4·61
Ni K	18·58
Zn K	10·32
Ag L	2·54
Sn L	63·96

Table 6 Energy dispersive spectroscopy analysis results of (I region in Fig. 6*b*) Sn–1·75Ag–4·5Zn solder on Ni plated Al substrate

	Positions
Elements	Region I, at-%
Al K	50·66
Ni K	21·88
Zn K	19·78
Ag L	1·81
Sn L	5·86

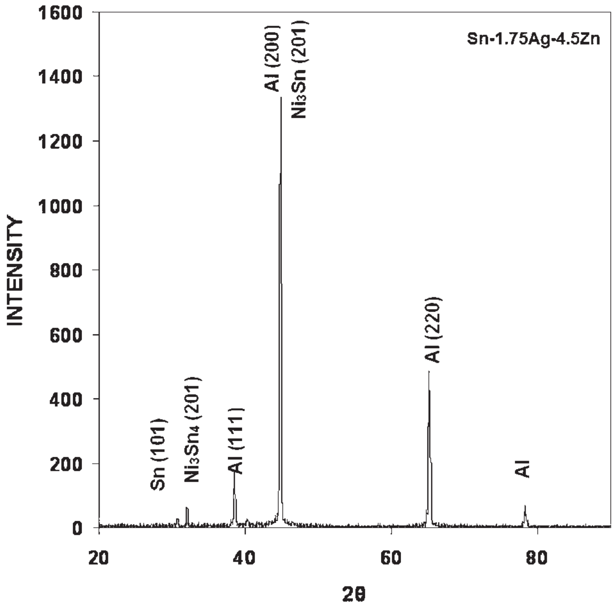

8 X-ray diffraction pattern of Sn–1·75Ag–4·5Zn/Ni coated Al interface

surrounding Ni_3Sn and Ni_3Sn_4 IMCs increased the viscosity of solidifying solder, decreasing its flowability. Hence, Sn–1·75Ag–4·5Zn solder exhibited poorer wettability compared to Sn–2·625Ag–2·25Zn. The Ni_3Sn_4 IMC strengthens the solder bond, but it decreases the fluidity property of solder. Hence, the wettabilities of both solders on Ni coated Al exhibit different behaviours.

Conclusions

High spreading rates (2–5° s^{-1}) were observed during spreading of solders in the initial 10–15 s, whereas the relaxation rates were negligible (<0·01° s^{-1}) after 1000 s. The Sn–2·625Ag–2·25Zn solder material exhibited better wettability compared to the Sn–1·75Ag–4·5Zn solder. The work of adhesion increased with decreasing surface roughness of substrates for both alloys. The contact angles obtained during spreading exhibited an increasing trend with increasing surface roughness for both solders. The Sn–2·625Ag–2·25Zn solder exhibited a thin continuous interface at the interface, and the Sn–1·75Ag–4·5Zn solder exhibited coarser interface with scallop shaped IMCs growing into the solder field. The difference in the wetting behaviour of two solders is caused by the variation in the type and morphology of IMC formed at the interface.

Acknowledgements

The authors acknowledge the help received from Dr G. Kumar, former PhD scholar, National Institute of Technology Karnataka, and now Associate Professor, Department of Mechanical Engineering, St Joseph Engineering College, Mangalore, for contact angle measurements. One of the authors (KNP) thanks the Defence Research Development Organisation, Government of India, New Delhi, for providing financial assistance for procurement of dynamic contact angle analyser.

References

1. G. Kumar and K. N. Prabhu: Proc. Int. Conf. on 'Advanced materials and composites', Trivandrum, India, October 2007, National Institute for Interdisciplinary Science and Technology, 535–540.
2. X. Wang, Y. C. Liu, C. Wei, L. M. Yu, Z. M. Gao and Z. Z. Dong: *Appl. Phys. A*, 2009, **96A**, 969–973.
3. R. A. Islam, Y. C. Chan, W. Jillek and S. Islam: *Microelectron. J.*, 2006, **37**, 705–713.
4. M. Kamal and E. S. Gouda: *J. Mater. Sci.: Mater. Electron.*, 2008, **19**, 81–84.
5. M. J. Rizvi, Y. C. Chan, C. Bailey, H. Lu, M. N. Islam and B. Y. Wu: *J. Electron. Mater.*, 2005, **34**, (8), 1115–1122.
6. X. R. Zhang, Z. F. Yuan, H. X. Zhao, L. K. Zang and J. Q. Li: *Chin. Sci. Bull.*, 2010, **55**, (9), 797–801.
7. H. H. Manko: 'Solder and soldering', 2nd edn; 1979, New York, McGraw-Hill.
8. Girish Kumar and K. N. Prabhu: *Adv. Colloid Interf. Sci.*, 2007, **133**, 61–89.
9. R. L. Xu, Y. C. Liu, Y. J. Han, C. Wei, X. Wang and L. M. Yu: *J. Mater. Sci.: Mater. Electron.*, 2009, **20**, 675–679.
10. Y.-Y. Chen and J.-G. Duh: *J. Mater. Sci.: Mater. Electron.*, 2000, **11**, 279–283.
11. Y. C. Liu, J. B. Wan and Z. M. Gao: *J. Alloys Compd*, 2008, **465**, 205–209.
12. J. B. Wan, Y. C. Liu, C. Wei, P. Jiang and Z. M. Gao: *J. Mater. Sci.: Mater. Electron.*, 2008, **19**, 1160–1168.
13. S. Amore, E. Ricci, G. Borzone and R. Novakovic: *Mater. Sci. Eng. A*, 2008, **A495**, 108–112.
14. G. Ghosh: *J. Electron. Mater.*, 2004, **33**, (10), 1080–1091.
15. D. C. Lin, R. Kovacevic, T. S. Srivatsan and G. X. Wang: *Sadhana*, 2008, **33**, (3), 251–259.
16. J. D. Dowd: 'Solders, fluxes, and techniques for soldering aluminum', STP 189-EB, ASTM, West Conshohocken, PA, USA, 1957, 5–13.
17. S. A. Vishenkov, V. M. Gostenina, V. S. Yekatova, I. A. Faykina and L. V. Filimonova: *Met. Sci. Heat Treat.*, 1962, **4**, 511–513.
18. http://www.boulder.nist.gov/div853/lead_free/part2.html#%202·2·19 18 (accessed 7 October 2010).
19. S. Shimada, Y. Takada, J. Lee and T. Tanka: *ISIJ Int.*, 2008, **48**, (9), 1246–1250.
20. V. I. Dybkov: *Solid State Phenom.*, 2008, **138**, 153–158.
21. W. K. Choi and H. M. Lee: *J. Electron. Mater.*, 1999, **28**, (11), 1251–1255.